Nuclear Instruments and Methods in Physics Research A274 (1989) 390–393
North-Holland, Amsterdam

FOCUSING PROPERTIES OF A BRAGG–FRESNEL LENS IN THE WHITE SPECTRUM OF SYNCHROTRON RADIATION

V.V. ARISTOV [1], Yu.A. BASOV [1], G.N. KULIPANOV [2], V.F. PINDYURIN [2], A.A. SNIGIREV [1] and A.S. SOKOLOV [2]

[1] *Institute of Problems of Microelectronics Technology and Superpure Materials, USSR Academy of Sciences, 142432 Chernogolovka, Moscow District, USSR*

[2] *Institute of Nuclear Physics, Siberian Division of the USSR, Academy of Sciences, 630090 Novosibirsk, USSR*

Received 9 February 1988 and in revised form 6 June 1988

Dedicated to Prof. U. Bonse on the occasion of his 60th birthday

Studies have been made of the peculiarities of image formation by a Bragg–Fresnel lens (BFL) in the white spectrum of synchrotron radiation (SR). Experimental results of focusing are obtained for different wavelengths. The results on focusing observed in an "anti-Bragg" geometry are given. The data obtained have been anlyzed.

Recent advances in diffraction physics and microstructuring technology have opened up possibilities for fabrication of focusing X-ray optical elements on the basis of perfect single crystals for the hard spectrum region ($\lambda \sim 1$ Å) [1–3] and on the basis of multilayer mirrors for soft X-rays ($10 < \lambda < 100$ Å) [4].

The effect of X-ray ($\lambda \sim 1$ Å) focusing by a perfect single crystal with a Fresnel zone structure artificially formed on its surface (a Bragg–Fresnel lens) was suggested and experimentally realized in refs. [1–3]. X-ray wave focusing was observed in a one-crystal scheme without preliminary monochromatization during diffraction on Si(111) planes (a conventional X-ray tube with a copper anode, $\lambda_{CuK\alpha} = 1.54$ Å, was used as a radiation source). In this connection of great interest is the investigation of the peculiarities of the formation of BFL diffraction contrast.

Experiments were performed using a synchrotron radiation beam emitted by a superconducting wiggler installed on the VEPP-2M, an electron–positron storage ring [5] (Novosibirsk, Institute of Nuclear Physics, Siberian Division of the USSR Academy of Sciences). Under typical experimental conditions the electron energy in the storage ring was 630 MeV, the maximum magnetic field on the axis of the wiggler 71 kG, the electron current in the storage ring 30 mA, the beam dimensions in the radiated region of the wiggler (dimensions of the radiation source) 60×800 μm^2. In all cases the distance between the radiation point and the BFL was $r_A = 5$ m. The SR beam came from the vacuum chamber of the storage ring through beryllium windows (the total thickness of Be was 200 μm). The latter prevented transmission of the long-wave part of the spectrum (the SR spectrum under typical experimental conditions is shown in fig. 1). Rectilinear zone plates fabricated from silicon single crystals by electron beam lithography and plasmachemical etching were used as a BFL. Fig. 2 shows one of these plates (reflecting Si(111) planes are parallel to the crystal surface): the zone height was 3 μm, exeeding the extinction depth value, the innermost zone width 20 μm, the outermost zone width 0.5 μm, the length 200 μm. The BFL is practically free from chromatic aberrations as compared with a conventional Fresnel zone plate.

In the experimental layout shown in fig. 3 X-ray focusing by a crystal lens was observed during 111-reflection from Si for different wavelengths (the angle of wave incidence on the crystal lens was varied in the experiment). Fig. 4 shows a number of photographs

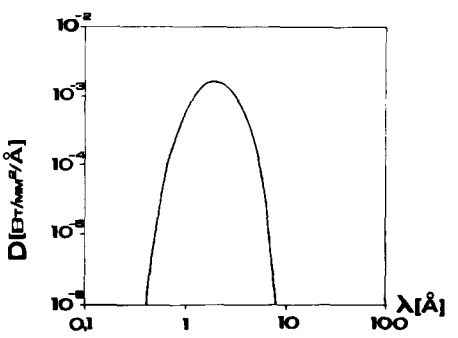

Fig. 1. SR spectral power density D of the VEPP-2M superconducting wiggler at a distance $r_A = 5$ m from the source.

0168-9002/89/$03.50

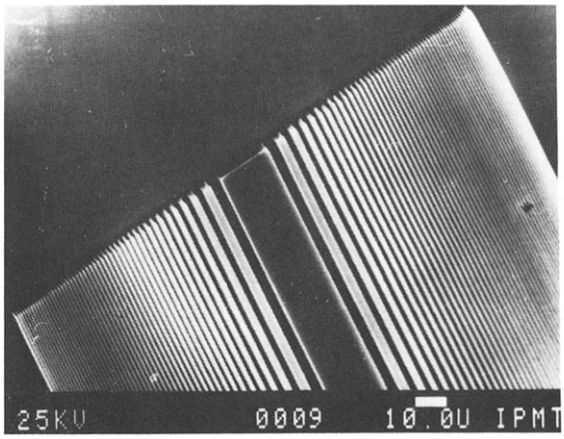

Fig. 2. Bragg–Fresnel lens.

recorded in the BFL focus ($r_A = 5$ m): (a) $\lambda = 1$ Å; $r_B = 2.7$ cm; (b) $\lambda = 1.73$ Å; $r_B = 4.4$ cm; (c) $\lambda = 2.5$ Å; $r_B = 6.5$ cm; where r_B is the BFL focal distance. It is readily seen from the images that the lens operates in a wide spectral range and the size of the focal spot is practically unaltered and equal to 2–3 μm (the diffraction pattern width alters with the variations in the BFL effective aperture). The size of the focal spot is determined by the resolution of the X-ray plate emulsion. It can be shown that in this geometry we can ignore chromatic widening since it equals $\sim 10^{-2}$ μm.

In the same experimental layout we also studied the changes in image contrast when passing from the region of a geometrical shadow through the focal plane into the region behind the focal plane. Fig. 5 shows a number of photographs corresponding to different r_B distances from the lens for $\lambda = 1.38$ Å: (a) 2.5 cm; (b) 3.5 cm; (c) 9 cm. At $r_B = 2.5$ cm (the region in front of the focal plane, fig. 5a). In the centre of the diffraction pattern there appears a maximum corresponding to Laue reflection from the BFL first zone (a lateral surface of the zone serves as an entrance slit). Under the

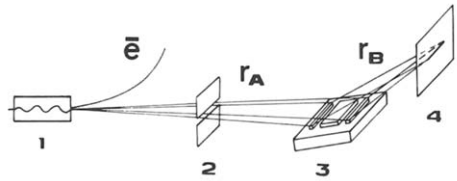

Fig. 3. Experimental layout: 1 – superconducting wiggler; 2 – slit; 3 – BFL; 4 – observation plane.

conditions of the experiment all the zones except the first (20 μm) one are smaller than the extinction depth for the Laue case ($\Lambda_L = 18$ μm), hence, the first zone makes the maximum contribution to Laue diffraction. The focusing conditions are fulfilled at $r_B = 3.5$ cm and the corresponding photograph (fig. 5b) shows a focused image of the radiation source in the centre of the diffraction pattern. The image in fig. 5 shows a contrast reversion in the region behind the focal plane which is known to be caused by a phase jump of the focusing wave field by π.

Up to now we have considered a focusing layout when the crystal surface is divided into Fresnel zones in the Bragg direction, i.e. in the diffraction plane. In the case of a cylindrical lens such a division can also be made in the direction perpendicular to the diffraction plane or, as we call it, in the "anti-Bragg" direction (see fig. 6). This can be easily done by rotating the BFL around the normal to the surface so that the generating line of the zone profile is parallel to the diffraction plane. In this case we have a phase lens (the X-ray absorption coefficient is close to zero when the Bragg conditions are fulfilled). With due regard to refraction, the optical path difference of the rays reflected from the lower and upper surfaces of the zone structure (fig. 7, on the left) is

$$\Delta = 2h \sin\theta + 2h \cos\theta \,\Delta\theta = 2h \sin\theta + \frac{\chi_0}{\sin\theta} h,$$

where χ_0 is the Fourier component of crystal polarizability. The first term can be neglected since it is a

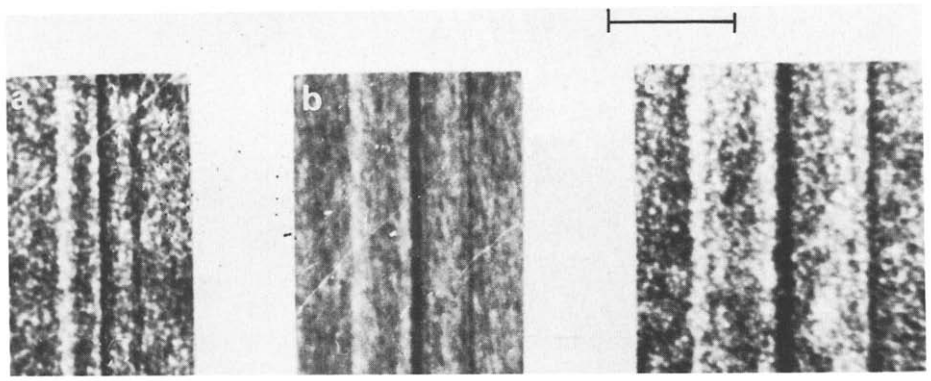

Fig. 4. Experimental X-ray photographs of focusing for different wavelengths: (a) $\lambda = 1$ Å; (b) $\lambda = 1.73$ Å; (c) $\lambda = 2.5$ Å. The marker bar indicates 50 μm.

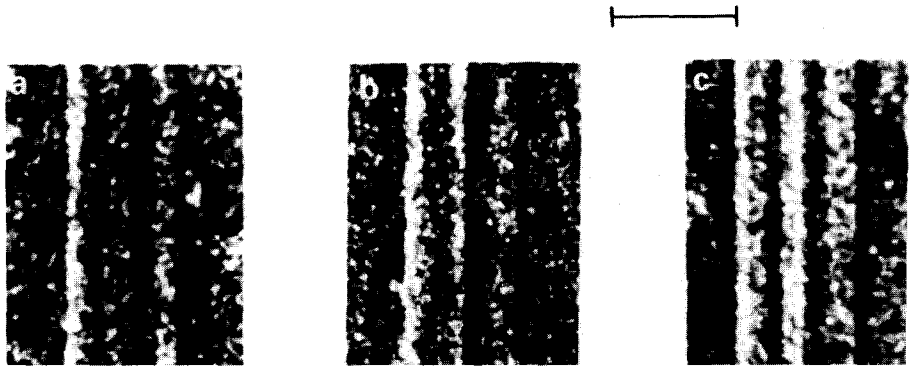

Fig. 5. Experimental X-ray photographs of the changes in image contrast when passing from the region of a geometrical shadow (a), through the focal plane (b), into the region behind the focal plane (c). The marker bar indicates 50 μm.

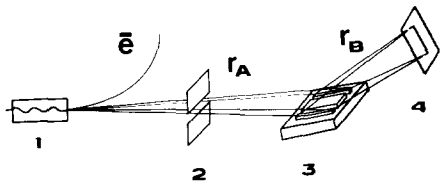

Fig. 6. Experimental scheme of focusing in "anti-Bragg" geometry: 1 – superconducting wiggler; 2 – slit; 3 – BFL; 4 – observation plane.

multiple of λ. Then the phase difference between these rays is determined by the second term and can be compared with the radiation wavelength. Here the phase shift is

$$\Delta\phi = \frac{2\pi}{\lambda}\frac{\chi_0}{\sin\theta}h = 4\pi d\frac{\chi_0}{\lambda^2}h,$$

where d is the crystal lattice period *. The value

* The following transformation shows that the phase shift here is determined on the extinction depth scale rather than on the wavelength scale:

$$\Delta\phi = \frac{2\pi}{\lambda}\frac{\chi_0}{\sin\theta}h = 2\chi_0 h\frac{\pi\chi_h}{\lambda\sin\theta}\frac{1}{\chi_h} = 2\frac{\chi_0}{\chi_h}\frac{h}{\Lambda_e},$$

where χ_h is the Fourier component of crystal polarizability.

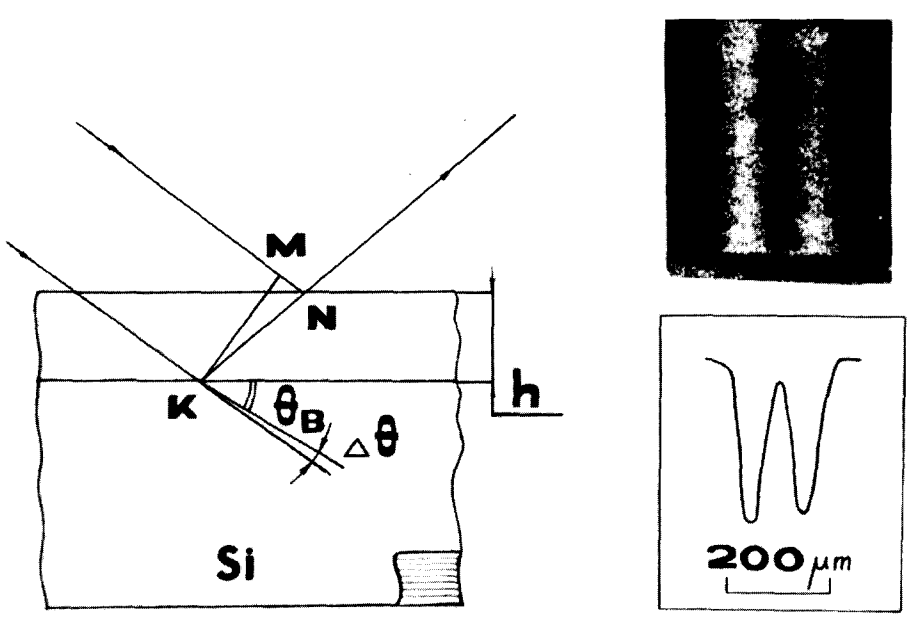

Fig. 7. X-ray focusing in "anti-Bragg" geometry: a scheme for the calculation of the optical path difference between the rays reflected from the lower and upper surfaces of a zone structure (on the left), an experimental image and a densitogram of focusing (on the right).

$(\chi_0/\lambda^2)d$ is constant for a specific reflection. Hence, the phase shift for this structure at a specific reflection is independent of the wavelength and determined only by the zone profile height h. The optimum value of the phase shift for obtaining a maximum radiation density in the focusing region should equal π.

Fig. 7 (on the right) shows an experimental photograph with an image of the source focus in the layout with "anti-Bragg" focusing: $r_A = 5$ m; $r_B = 0.4$ m; $\lambda = 2.5$ Å; Si(111) reflection. The size of the focused image equals 70 μm and, hence, with regard to the reduction coefficient the source size should be: $\delta_s = (r_A/r_B)$ 70 μm = 875 μm, which follows the size of the radiating region. It should be noted that in this case the focusing efficiency is 2%, i.e. the phase shift in the experiment was equal to 0.4π.

At an optimum height of the structure a focusing efficiency of up to 40% can be obtained for a rectangular zone profile and up to 100% for a kinoform lens (sawtooth profile) *.

The focusing elements of X-ray optics (cylinder and sphere-shaped crystals) used in SR experiments exhibit a low spatial resolution (~ 0.1 mm) and a low thermal stability (radiation heating of the crystal changes its bending radius). A Bragg–Fresnel lens used as a focusing element permits obtaining a spatial resolution of the order of 0.1 μm and, moreover, this optics displays thermal stability. Thus, focusing elements, namely, Bragg–Fresnel lenses, enable one to solve the problem of creating effective and high resolution X-ray optics for synchrotron experiments.

* The term "kinoform" was first introduced in ref. [6] and is widely used now in optical holography.

Acknowledgements

We would like to thank A.Yu. Suvorov for his help in performing the experiment. We are also grateful to the staff of the VEPP-2M for providing stable operation of the system during the experiments.

References

[1] V.V. Aristov, A.A. Snigirev, Yu,A. Basov and A.Yu. Nikulin, AIP Conf. Proc. 147 (1986) 253.
[2] V.V. Aristov, Yu.A. Basov and A.A. Snigirev, Pis'ma Zh. Tekh. Fiz. 13 (1987) 114.
[3] V.V. Aristov, Yu.A. Basov, S.V. Redkin, A.A. Snigirev and V.A. Yunkin, Nucl. Instr. and Meth. A261 (1987) 72.
[4] V.V. Aristov, S.V. Gaponov, V.M. Geshkin, Yu.A. Gorbatov, A.I. Erko, V.V. Martynov, L.A. Matveeva, N.N. Salachshenko and A.A. Fraerman, Pis'ma Zh. Eksp. Teor. Fiz. 44 (1986) 207.
[5] E.S. Gluskin, P.M. Ivanov, G.N. Kulipanov, A.N. Skrinsky and Yu.M. Shatunov, Nucl. Instr. and Meth. A246 (1986) 41.
[6] L.B. Lesem, P.M. Hirsch and J.A. Jordan, IBM J. Res. Develop. 13 (1969) 150.